

Electrochemical performance of LiFePO₄/C doped with F synthesized by carbothermal reduction method using NH₄F as dopant

Maosen Pan · Xuehao Lin · Zhentao Zhou

Received: 3 May 2011 / Revised: 23 September 2011 / Accepted: 25 September 2011 / Published online: 18 October 2011
© Springer-Verlag 2011

Abstract The effect of fluorine doping on the electrochemical performance of LiFePO₄/C cathode material is investigated. The stoichiometric proportion of LiFe(PO₄)_{1-x}F_{3x}/C ($x=0.01, 0.05, 0.1, 0.2$) materials was synthesized by a solid-state carbothermal reduction route at 650 °C using NH₄F as dopant. X-ray diffraction, scanning electron microscope, energy-dispersive X-ray, and X-ray photoelectron spectroscopy analyses demonstrate that fluorine can be incorporated into LiFePO₄/C without altering the olivine structure, but slightly changing the lattice parameters and having little effect on the particle sizes. However, heavy fluorine doping can bring in impurities. Fluorine doping in LiFePO₄/C results in good reversible capacity and rate capability. LiFe(PO₄)_{0.95}F_{0.15}/C exhibits highest initial capacity and best rate performance. Its discharge capacities at 0.1 and 5 C rates are 156.1 and 119.1 mAh g⁻¹, respectively. LiFe(PO₄)_{0.95}F_{0.15}/C also presents an obviously better cycle life than the other samples. We attribute the improvement of the electrochemical performance to the smaller charge transfer resistance (R_{ct}) and influence of fluorine on the PO₄³⁻ polyanion in LiFePO₄/C.

Keywords Electrochemical performance · Carbothermal reduction method · Ammonium fluoride · F-doped lithium iron phosphate · Dopant

M. Pan · Z. Zhou (✉)
College of Materials Science and Engineering,
South China University of Technology,
Guangzhou 510640, People's Republic of China
e-mail: mcztzhou@scut.edu.cn

M. Pan
e-mail: p_ms@163.com

X. Lin
Shenzhen Meixin Electronics Co. Ltd,
Shenzhen 518000, People's Republic of China

Introduction

Olivine-typed LiFePO₄ has attracted much attention in the past decades because of its low toxicity, low cost, high safety, and excellent reversibility of electrochemistry [1]. However, the low electronic and ion conductivities of pristine LiFePO₄ result in poor electrochemical performance especially under moderate and high rates, which poses a great challenge for its practical applications such as electric vehicles and hybrid electric vehicles [2]. So, numerous methods, mainly including carbon coating [3–5], particle size reduction [6, 7], and heteroatom doping [2, 8–11], have been developed to overcome these drawbacks.

In recent years, anion doping has been considered as an established approach to improve the electrochemical performance of LiFePO₄ cathode material [11–15]. Especially, fluorine doping at the oxygen site or substituting for PO₄³⁺ polyanion can improve obviously the rate capability and cyclic performance [12, 13]. Unfortunately, their research results show that some impurities such as LiF and Fe₂(PO₄)F existing in the LiFePO₄ product which could cause a capacity loss and fluorine waste. Moreover, the LiF dopant was generally regarded as a stable compound even at high temperature [16]. Compared with LiF, NH₄F is not only facily decomposed at lower temperature but also cheaper. What is more, it also can be completely utilized. Therefore, NH₄F is preferred to be used as F dopant.

On the other hand, synthesis route significantly affects the cathode material's electrochemical performance and the cost [17, 18]. Recently, the solid-state carbothermal reduction (CTR) method has been successfully applied in the preparation of LiFePO₄ [17–20]. This method has many advantages, such as low cost of raw material and simple

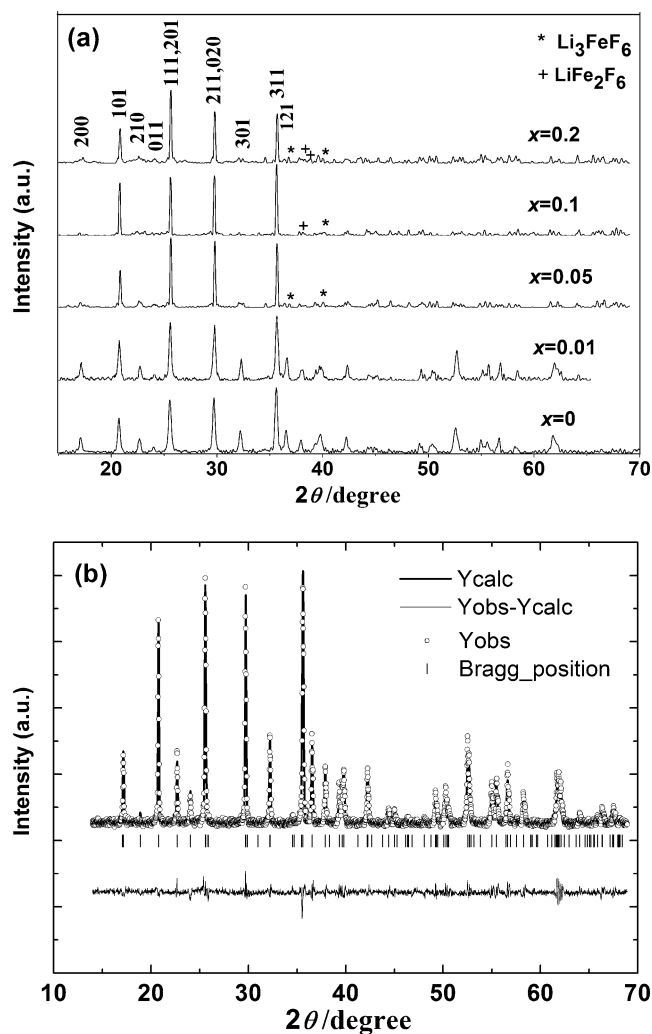


Fig. 1 **a** XRD patterns of $\text{LiFe}(\text{PO}_4)_{1-x}\text{F}_{3x}/\text{C}$ ($x=0.01, 0.05, 0.1, 0.2$) materials and **b** the Rietveld refinement of $\text{LiFe}(\text{PO}_4)_{0.95}\text{F}_{0.15}/\text{C}$

synthesis process. However, there is no literature about it being used in the synthesis of F-doped LiFePO_4 material. In this investigation, we prepared the $\text{LiFe}(\text{PO}_4)_{1-x}\text{F}_{3x}/\text{C}$ ($x=0, 0.01, 0.05, 0.1, 0.2$) cathode materials by CTR method using NH_4F as the dopant, and the effect of fluorine doping on the electrochemical performance of LiFePO_4/C cathode material was studied in details.

Table 1 The lattice parameters and refinement factors of the samples with different fluorine content

F content ^a	$a/\text{\AA}$	$b/\text{\AA}$	$c/\text{\AA}$	$V/\text{\AA}^3$	R_p (%)	R_{wp} (%)
0	10.3298	6.0059	4.6974	291.43	5.24	4.08
0.01	10.3327	6.0058	4.6953	291.37	6.31	4.97
0.05	10.3320	5.9852	4.6942	290.29	8.57	6.71
0.1	10.3356	6.0028	4.6949	291.28	9.63	8.32
0.2	10.3373	6.0104	4.6955	291.74	11.46	10.05

^aF content is the variable x in the formula of $\text{LiFe}(\text{PO}_4)_{1-x}\text{F}_{3x}/\text{C}$ ($0 \leq x < 0.5$)

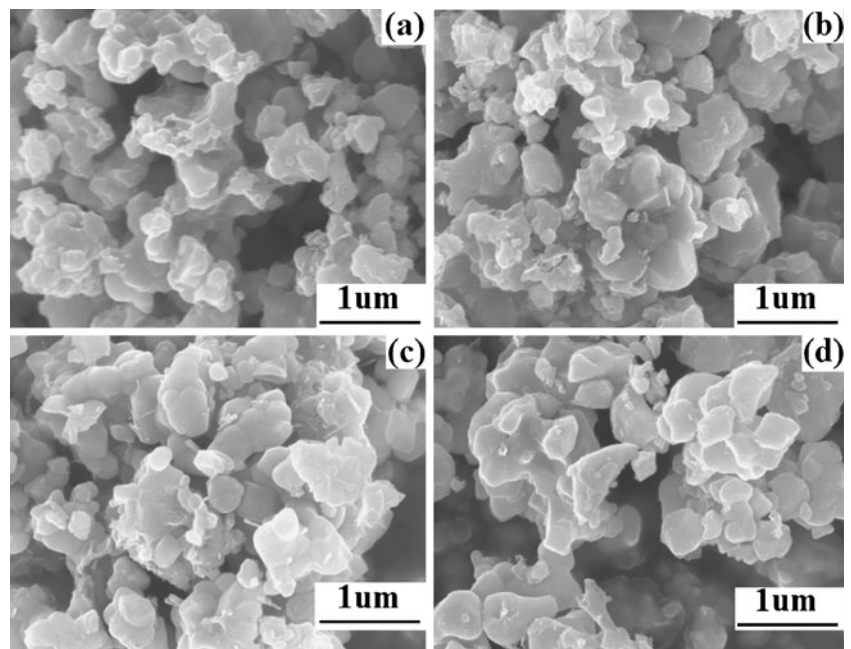
Experimental

$\text{LiFe}(\text{PO}_4)_{1-x}\text{F}_{3x}/\text{C}$ ($x=0, 0.01, 0.05, 0.1, 0.2$) materials were synthesized by a solid-state CTR route of stoichiometric amount of Fe_2O_3 , $(\text{NH}_4)_2\text{HPO}_4$, Li_2CO_3 , and NH_4F , using soluble starch (25.0 g starch/1 mol Fe_2O_3) as reducing agent and carbon source. The starting materials were mixed by planetary ball-milling for 6 h in ethanol absolute medium. The resulting mixture was heated at a rate of $1^\circ\text{C}/\text{min}$ to 300°C and kept for 10 h, followed by sintering at 650°C for 24 h. The whole heating procedure was under nitrogen atmosphere. After the temperature was cooled down to room atmosphere, the products were ground by hand until the powder size was below 400 meshes. Finally, $\text{LiFe}(\text{PO}_4)_{1-x}\text{F}_{3x}/\text{C}$ samples ($x=0, 0.01, 0.05, 0.1, 0.2$) were obtained. The carbon content in the $\text{LiFe}(\text{PO}_4)_{1-x}\text{F}_{3x}/\text{C}$ ($x=0, 0.01, 0.05, 0.1, 0.2$) powder is about 5.4 (± 0.2) wt.% as determined by a chemical analysis [21].

The samples were verified by powder X-ray diffraction (XRD; Bruker D8 ADVANCE, Germany) using $\text{Cu K}\alpha$ radiation. The morphology and microstructure of this material were observed by scanning electron microscope (SEM; LEO-1530VP, Germany). Energy-dispersive X-ray analysis (EDX) was performed by using a Roentec EDX detector mounted on the LEO-1530VP scanning electron microscope. X-ray photoelectron spectroscopy (XPS) was obtained for the LiFePO_4/C and $\text{LiFe}(\text{PO}_4)_{0.95}\text{F}_{0.15}/\text{C}$ under Kratos Axis Ultra DLD spectrometer with monochromatic $\text{Al K}\alpha$ radiation ($h\nu=1,486.6$ eV).

Electrochemical testing was performed by assembling coin-typed cells with a cathode and a lithium foil anode separated by a Celguard 2300 micro-porous membrane and with 1 M LiPF_6 in 1:1 ethylene carbonate/dimethyl carbonate as electrolyte. For cathode fabrication, the as-synthesized $\text{LiFe}(\text{PO}_4)_{1-x}\text{F}_{3x}/\text{C}$ ($x=0, 0.01, 0.05, 0.1, 0.2$) was mixed with acetylene black and polytetrafluoroethylene binder with a weight ratio of 85:10:5. Then, the mixture was pressed onto a stainless mesh (current collector) and dried at 120°C for 24 h in a vacuum oven. The assembly of the cell was carried out in a dry N_2 -filled glove box. The charge and discharge test of the cells were examined by a Qintian BS-9300 electrochemical test

Fig. 2 SEM images of LiFe(PO₄)_{1-x}F_{3x}/C materials: **a** $x=0.01$, **b** $x=0.05$, **c** $x=0.1$, **d** $x=0.2$



instrument between 2.5 and 4.2 V at an ambient temperature. Cyclic voltammetry (CV) measurements and electrochemical impedance spectroscopy (EIS) were performed on a CHI660B (Chenhua, Shanghai) electrochemical workstation. The scan rate of CV was 0.1 mV s⁻¹ over a voltage range of 2.5–4.2 V while the amplitude of EIS was 5 mV in the frequency range of 10⁻²–10⁵ Hz.

Results and discussion

Figure 1 shows the XRD patterns of LiFe(PO₄)_{1-x}F_{3x}/C ($x=0, 0.01, 0.05, 0.1, 0.2$) samples and the Rietveld refinement of LiFe(PO₄)_{0.95}F_{0.15}/C. The main diffraction peaks of these materials can be indexed to LiFePO₄ with an ordered olivine structure (orthorhombic *Pnmb* group given by

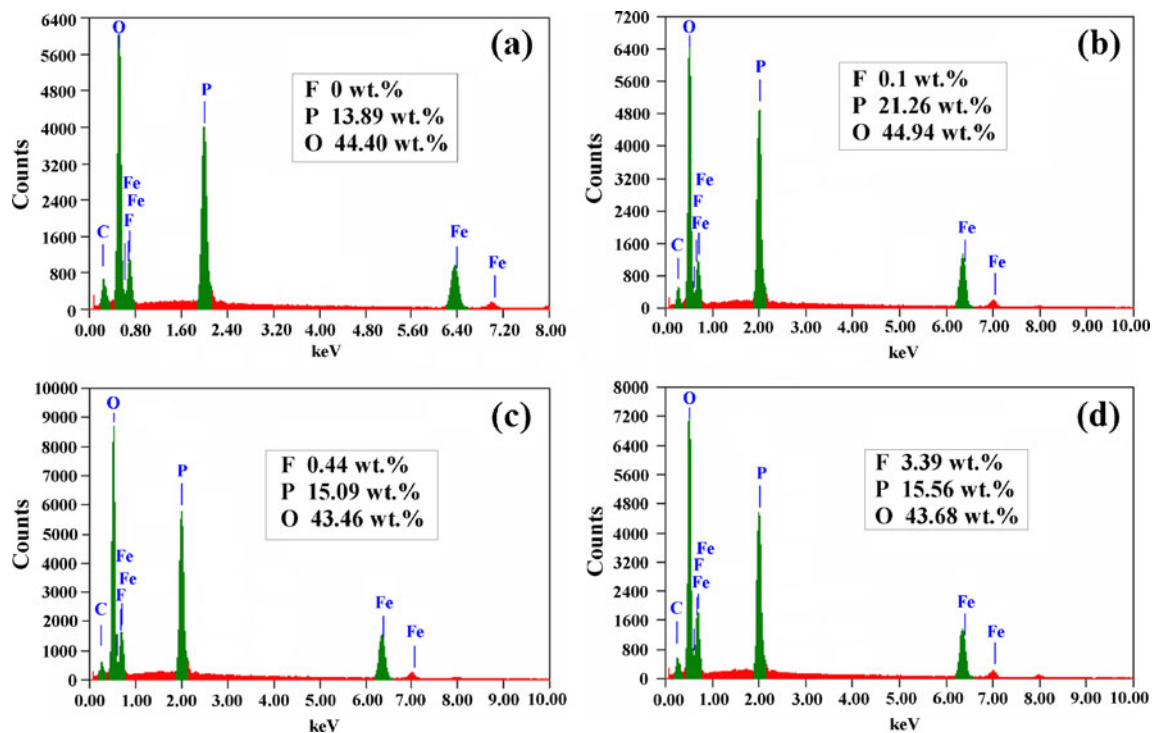


Fig. 3 EDX analysis of LiFe(PO₄)_{1-x}F_{3x}/C materials: **a** $x=0.01$, **b** $x=0.05$, **c** $x=0.1$, **d** $x=0.2$

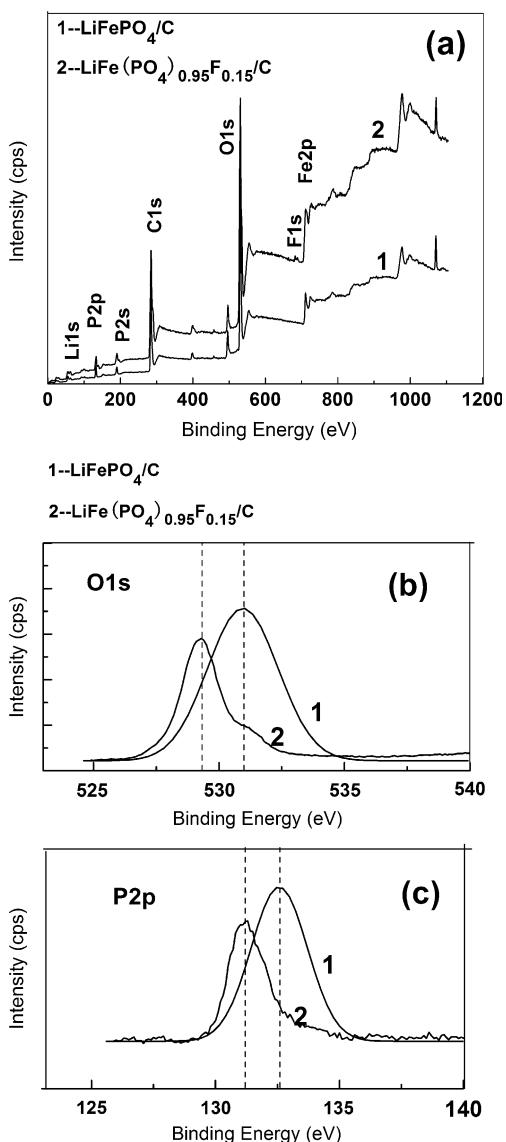


Fig. 4 XPS spectra of $\text{LiFe}(\text{PO}_4)_{1-x}\text{F}_{3x}/\text{C}$ ($x=0, 0.05$) materials: **a** wide-range scanning spectrum; high resolution spectra of **b** O and **c** P

JCPDS 83–2092). The diffraction peaks varied obviously with the increase of F content added in LiFePO_4/C composite, namely, the location of which shifting to the higher or lower 2θ angles as well as the fading of weak diffraction peaks (seen in Fig. 1a). Even some impurities such as Li_3FeF_6 and LiFe_2F_6 appeared when the fluorine content was more than 0.05. The refined lattice parameters of five samples were obtained by Rietveld method, as shown in Table 1, and the Rietveld profile refinement of the typical sample of $\text{LiFe}(\text{PO}_4)_{0.95}\text{F}_{0.15}/\text{C}$ was presented in Fig. 1b. It can be seen from Table 1 that the lattice parameters decreased with the increase of F content up to 0.05. However, a further increase of the F content resulted in the increase of lattice parameters. The refinement factors of the samples except $\text{LiFe}(\text{PO}_4)_{0.8}\text{F}_{0.6}/\text{C}$ were lower than

10%, which indicated the reliance of the refinement data. All of the above results suggest that fluorine has been successfully incorporated into the lattice of LiFePO_4/C without altering its olivine structure, but slightly changing the lattice parameters [9, 12].

The morphology of $\text{LiFe}(\text{PO}_4)_{1-x}\text{F}_{3x}/\text{C}$ ($x=0.01, 0.05, 0.1, 0.2$) materials are shown in Fig. 2. It can be seen that the F-doped LiFePO_4/C materials had the sphere-like surface, the particle sizes of which were about 250–400 nm. The content of fluorine introduced into the LiFePO_4/C matrix structure has little effect on the growth of the particle sizes.

In order to clarify F distribution on the surfaces of $\text{LiFe}(\text{PO}_4)_{1-x}\text{F}_{3x}/\text{C}$ ($x=0.01, 0.05, 0.1, 0.2$) materials, energy-dispersive X-ray analysis was used to scan the samples. The results are shown in Fig. 3. From the EDX spectra, it can be estimated that the F content of $\text{LiFe}(\text{PO}_4)_{1-x}\text{F}_{3x}/\text{C}$ ($x=0.01, 0.05, 0.1, 0.2$) materials was about 0, 0.1, 0.44 and 3.39 wt. %, while the corresponding P/O ratios were 0.162, 0.244, 0.179, and 0.185, respectively. These data indicate that F element exists in these $\text{LiFe}(\text{PO}_4)_{1-x}\text{F}_{3x}/\text{C}$ ($x=0.05, 0.1, 0.2$) materials. More importantly, the P/O ratio of $\text{LiFe}(\text{PO}_4)_{0.95}\text{F}_{0.15}/\text{C}$ composite is nearest approach to the ideal state of LiFePO_4 (its P/O ratio is 0.25, namely, one P atom combining with four O atoms in LiFePO_4 formula), which means that the destruction of fluorine to the PO_4^{3-} polyanion in LiFePO_4 formula can be reduced to the lowest level when the F content was about 0.05. This point is very important for the F-doped LiFePO_4/C cathode material to get good electrochemical performance.

To get more information about the substitution of fluorine, the binding energy of oxygen and phosphorous ions in both LiFePO_4/C and $\text{LiFe}(\text{PO}_4)_{0.95}\text{F}_{0.15}/\text{C}$ was investigated by XPS. The results were exhibited in Fig. 4. From Fig. 4a, it can be found that one F_{1s} peak centered at 682.7 eV appeared in the wide-range scanning spectra of $\text{LiFe}(\text{PO}_4)_{0.95}\text{F}_{0.15}/\text{C}$, while only Li, Fe, P, O, and C element existed in the sample LiFePO_4/C . This indicates

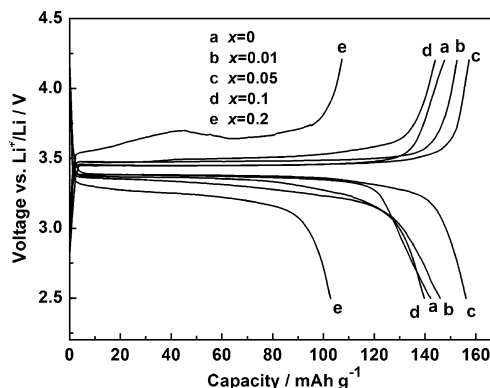
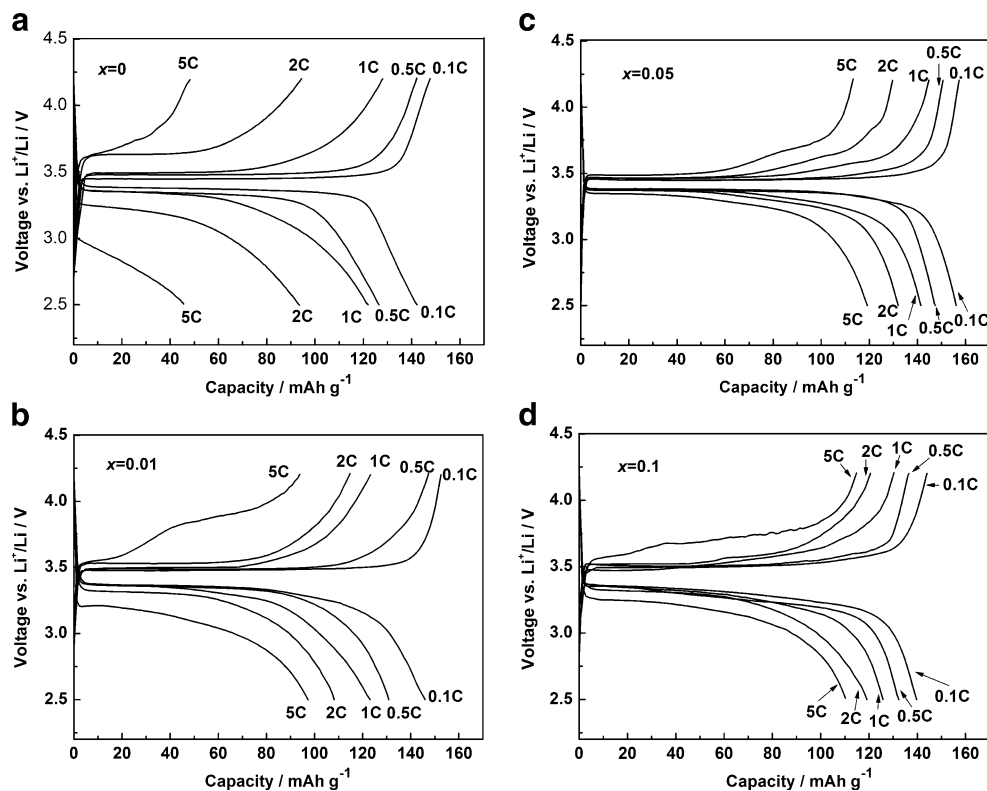


Fig. 5 Charge–discharge curves of $\text{LiFe}(\text{PO}_4)_{1-x}\text{F}_{3x}/\text{C}$ ($x=0, 0.01, 0.05, 0.1, 0.2$) materials at 0.1 C rate

Fig. 6 Charge–discharge profiles of $\text{LiFe}(\text{PO}_4)_{1-x}\text{F}_{3x}/\text{C}$ materials: **a** $x=0$, **b** $x=0.01$, **c** $x=0.05$, **d** $x=0.1$ at 0.1–5 C rates



introduction of fluorine into the LiFePO_4/C . More interesting things happened in the high-resolution spectra of O and P (Fig. 4b, c). Not only the O_{1s} peak but also the P_{2p} peak of $\text{LiFe}(\text{PO}_4)_{0.95}\text{F}_{0.15}/\text{C}$ had a chemical shift compared to that of LiFePO_4/C . This suggests the influence of fluorine incorporated into LiFePO_4/C on both O and P element, namely, the PO_4^{3-} polyanion of LiFePO_4/C . Therefore, we concluded that fluorine substituted for PO_4^{3-} polyanion of LiFePO_4/C .

Figure 5 presents the charge–discharge profiles of $\text{LiFe}(\text{PO}_4)_{1-x}\text{F}_{3x}/\text{C}$ ($x=0, 0.01, 0.05, 0.1, 0.2$) at 0.1 C (1 C = 170 mA g^{-1}) rate. F-doped LiFePO_4/C materials remained in the same shape of charge–discharge profiles as the undoped one. The $\text{LiFe}(\text{PO}_4)_{0.95}\text{F}_{0.15}/\text{C}$ material delivered the highest discharge capability of 156.1 mAh g^{-1} among all of the samples, and the other samples $\text{LiFe}(\text{PO}_4)_{1-x}\text{F}_{3x}/\text{C}$ ($x=0, 0.01, 0.1, 0.2$) showed a capacity of 142.2, 146.0, 139.7, and 102.8 mAh g^{-1} , respectively. It can be seen that the reversible capacities of these cathode materials increased with the increase in fluorine content. However, excess fluorine in the LiFePO_4/C powder caused a capacity loss due to the appearance of impurities and the influence of fluorine on the PO_4^{3-} polyanion. These data suggest that fluorine introduced into LiFePO_4/C improves the reversible capacity of the cathode materials, but the fluorine content needs to be controlled to some extent.

Figure 6 compares the rate performance of $\text{LiFe}(\text{PO}_4)_{1-x}\text{F}_{3x}/\text{C}$ ($x=0, 0.01, 0.05, 0.1$) samples at 0.1–5 C rates.

Both charge and discharge performances of LiFePO_4/C were strongly affected by charge and discharge rates. The discharge voltage plateau decreased obviously from 3.37 V (0.1 C) to 2.8 V (5 C) with increased C rates, while the charge voltage plateau increased from 3.45 V (0.1 C) to 3.8 V (5 C). Both charge and discharge capacities also faded sharply when the C rates increased. Even at 5 C rates, its discharge capacity decreased to 45.6 mAh g^{-1} . On the other hand, F-doped LiFePO_4/C materials showed higher initial discharge voltage and lower charge voltage than the undoped one under all charge and discharge rates. Furthermore, reversible capacities also were improved greatly, especially when the rate was above 2 C. This indicates that

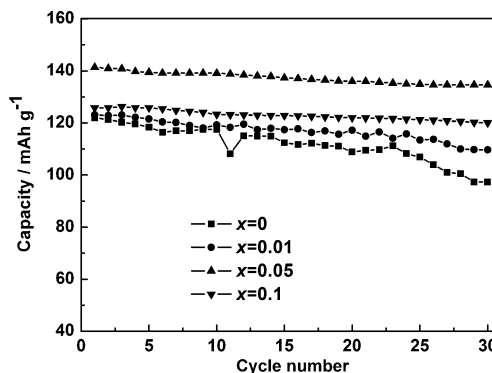


Fig. 7 Cycle performance of $\text{LiFe}(\text{PO}_4)_{1-x}\text{F}_{3x}/\text{C}$ ($x=0, 0.01, 0.05, 0.1$) materials at 1 C rate

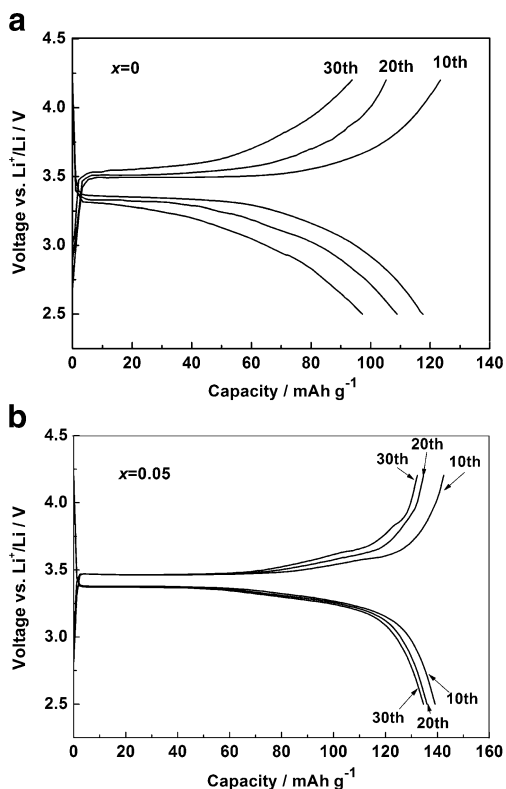


Fig. 8 Charge–discharge profiles of $\text{LiFe}(\text{PO}_4)_{1-x}\text{F}_{3x}/\text{C}$ materials: **a** $x=0$, **b** $x=0.05$ at 1 C rate

fluorine doping improves the ion conductivities of these cathode materials and alleviates its polarizations. It should be noticed that the $\text{LiFe}(\text{PO}_4)_{0.95}\text{F}_{0.15}/\text{C}$ material exhibited the best electrochemical performance among all the F-doped LiFePO_4/C materials. Its discharge capacity at 0.1, 0.5, 1, 2, and 5 C rates was 156.1, 147.5, 141.4, 132.0, and 119.1 mAh g^{-1} , respectively. The charge and discharge voltage varied from 3.45 V (0.1 C) to 3.55 V (5 C) and from 3.38 V (0.1 C) to 3.3 V (5 C), respectively. Comparably, the discharge capacity of $\text{LiFe}(\text{PO}_4)_{0.99}\text{F}_{0.03}/\text{C}$ at 0.1, 0.5, 1, 2, and 5 C was 146.0, 130.9, 123.1, 108.1, and 97.3 mAh g^{-1} ,

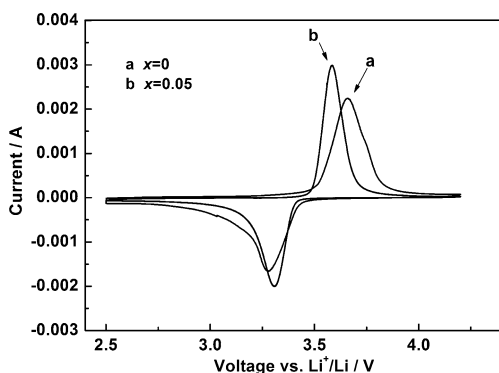


Fig. 9 Cyclic voltammety curves of $\text{LiFe}(\text{PO}_4)_{1-x}\text{F}_{3x}/\text{C}$ ($x=0, 0.05$) materials

respectively, while 139.7, 132.3, 125.8, 119.1, and 110.2 mAh g^{-1} for the $\text{LiFe}(\text{PO}_4)_{0.99}\text{F}_{0.03}/\text{C}$. Both of them showed significant polarization, which resulted in lower discharge voltage and higher charge voltage than the $\text{LiFe}(\text{PO}_4)_{0.95}\text{F}_{0.15}/\text{C}$ sample. The reason for this can be attributed to two aspects. One is the shortage or excess of fluorine. The shortage of fluorine cannot afford enough F^- that improves the motion of lithium ions [9, 12]. By contrary, the excess of fluorine would produce impurities (confirmed by the XRD in Fig. 1), which were inactive in the cathode materials. It should be pointed out that a few impurities had no effect on the electrochemical performance of the F-doped LiFePO_4/C material, such as $\text{LiFe}(\text{PO}_4)_{0.95}\text{F}_{0.15}/\text{C}$. The other aspect is the influence of fluorine on the PO_4^{3-} polyanion in the LiFePO_4/C material. $\text{LiFe}(\text{PO}_4)_{0.95}\text{F}_{0.15}/\text{C}$ material has the perfect P/O ratio (namely, a little damage to the PO_4^{3-} polyanion). Consequently, $\text{LiFe}(\text{PO}_4)_{0.95}\text{F}_{0.15}/\text{C}$ material shows the best electrochemical performance.

Figure 7 exhibits the cycling characteristics of $\text{LiFe}(\text{PO}_4)_{1-x}\text{F}_{3x}/\text{C}$ ($x=0, 0.01, 0.05, 0.1$) materials at 1 C rate for 30 cycles. It is easy to find that the $\text{LiFe}(\text{PO}_4)_{0.99}\text{F}_{0.03}/\text{C}$ sample has a similar cycle stability to the un-doped LiFePO_4/C material. The other samples, $\text{LiFe}(\text{PO}_4)_{0.95}\text{F}_{0.15}/\text{C}$ and $\text{LiFe}(\text{PO}_4)_{0.9}\text{F}_{0.3}/\text{C}$, presented obviously better cycle life and higher cycling capacity than that of the un-doped one. The capacity of 30th cycle for the $\text{LiFe}(\text{PO}_4)_{1-x}\text{F}_{3x}/\text{C}$ ($x=0, 0.01, 0.05, 0.1$) samples was 97.3, 109.7, 134.6, and 120.0 mAh g^{-1} , respectively. After 30 cycles, the capacity retention of LiFePO_4/C was only 79.8% of the initial capacity. However, the $\text{LiFe}(\text{PO}_4)_{1-x}\text{F}_{3x}/\text{C}$ ($x=0.01, 0.05, 0.1$) materials kept 89.1%, 95.2%, and 95.4% of the initial capacity, respectively. This indicates that fluorine doping does not change the olivine structure of LiFePO_4/C but enhances its cycling performance. In order to know more details about the cycling performance of $\text{LiFe}(\text{PO}_4)_{0.95}\text{F}_{0.15}/\text{C}$ sample, voltage profiles from cycles 10, 20, and 30 for LiFePO_4/C and $\text{LiFe}(\text{PO}_4)_{0.95}\text{F}_{0.15}/\text{C}$ were compared in Fig. 8. It is clear to observe that the charge–discharge profiles of $\text{LiFe}(\text{PO}_4)_{0.95}\text{F}_{0.15}/\text{C}$ material main-

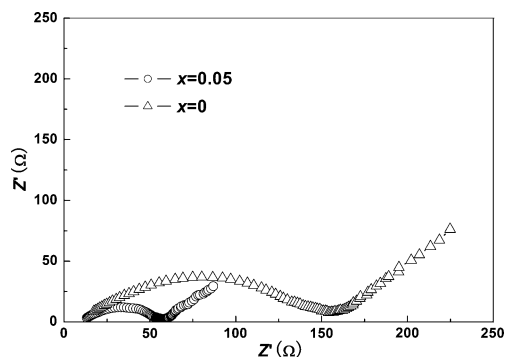


Fig. 10 EIS spectra of $\text{LiFe}(\text{PO}_4)_{1-x}\text{F}_{3x}/\text{C}$ ($x=0, 0.05$) materials

tained almost the same shape after 30 cycles. The capacity also faded slowly. However, the curves of LiFePO_4/C changed greatly with the cycles. Significant polarization happened after 10 cycles and the voltage polarization became more severe as the cycling proceeded. Besides, the capacity of LiFePO_4/C decreased sharply with the cycling. All these results suggest that fluorine doped in LiFePO_4/C reduced both inner resistance and voltage polarization of these cathode materials, which resulted in good cycling performance of the cells.

In order to have a further study on the effect of fluorine on the electrochemical performance of LiFePO_4/C and $\text{LiFe}(\text{PO}_4)_{0.95}\text{F}_{0.15}/\text{C}$, cyclic voltammetry was carried out. The CV curves of $\text{LiFe}(\text{PO}_4)_{1-x}\text{F}_{3x}/\text{C}$ ($x=0, 0.05$) samples are shown in Fig. 9. It can be observed that the two samples have similar redox peaks. The redox peaks of $\text{LiFe}(\text{PO}_4)_{0.95}\text{F}_{0.15}/\text{C}$ and LiFePO_4/C were centered at 3.585/3.309 and 3.656/3.281 V, respectively. Obviously, the peak separation of $\text{LiFe}(\text{PO}_4)_{0.95}\text{F}_{0.15}/\text{C}$ was narrower and the peak shape was sharper than that of LiFePO_4/C . These results demonstrate that easier lithium insertion and extraction happened in the $\text{LiFe}(\text{PO}_4)_{0.95}\text{F}_{0.15}/\text{C}$ material.

Figure 10 presents the Nyquist plots for $\text{LiFe}(\text{PO}_4)_{1-x}\text{F}_{3x}/\text{C}$ ($x=0, 0.05$) materials. The intercept to real axis at the high frequency end of semicircle corresponds to the electrolyte ions transportation barrier (R_e). The high frequency semicircle is related to the charge transfer process, the diameter of which is equal to the charge transfer resistance (R_{ct}). The low frequency straight line predicts a typical Warburg behavior that provides the Li^+ diffusion process from the surface to the interior of the crystalline $\text{LiFe}(\text{PO}_4)_{1-x}\text{F}_{3x}/\text{C}$. The R_e of both samples are about 13–17 Ω . The R_{ct} of F-doped material is ca. 44 Ω , much lower than that of the un-doped one (ca. 137 Ω). This indicates that F-doping reduced the R_{ct} , namely, increasing the conductivity of the LiFePO_4/C material. Therefore, the kinetics of the charge–discharge process was improved, resulting in good electrochemical performance.

Conclusions

In summary, $\text{LiFe}(\text{PO}_4)_{1-x}\text{F}_{3x}/\text{C}$ ($x=0.01, 0.05, 0.1, 0.2$) cathode materials were synthesized by a CTR method at 650 °C using NH_4F as dopant. XRD, SEM, EDX, and XPS analyses demonstrated that fluorine could be incorporated into LiFePO_4/C without altering the olivine structure but slightly changing the lattice parameters and having little

effect on the particle sizes. However, heavy fluorine (F content was more than 0.05) brought in impurities. Fluorine doping can improve the reversible capacity and rate capability of the cathode materials. $\text{LiFe}(\text{PO}_4)_{0.95}\text{F}_{0.15}/\text{C}$ exhibited highest initial capacity and best rate performance. Its discharge capacities at 0.1 and 5 C rates were 156.1 and 119.1 mAh g^{-1} , respectively. $\text{LiFe}(\text{PO}_4)_{0.95}\text{F}_{0.15}/\text{C}$ also presented obviously better cycle life than the other samples. All of these are mainly attributed to the smaller charge transfer resistance (R_{ct}) and influence of fluorine on the PO_4^{3-} polyanion in LiFePO_4/C .

Acknowledgement The authors wish to thank Guangzhou Tianci High-tech Materials Co. Ltd. for the electrolyte.

References

1. Padhi AK, Nanjundaswamy KS, Goodenough JB (1997) *J Electrochem Soc* 144:1188–1194
2. Sun CS, Zhou Z, Xu ZG, Wang DG, Wei JP, Bian XK, Yan J (2009) *J Power Sources* 193:841–845
3. Wilcox JD, Doeff MM, Marcinek M, Kostecki R (2007) *J Electrochem Soc* 154:A389–395
4. Pan M, Zhou Z (2011) *Mater Lett* 65:1131–1133
5. Huang Y, Ren H, Yin S, Wang Y, Peng Z (2010) *J Power Sources* 195:610–613
6. Gaberscek M, Dominko R, Jamnik J (2007) *Electrochem Commun* 9:2778–2783
7. Zheng JC, Li XH, Wang ZX, Guo HJ, Zhou SY (2008) *J Power Sources* 184:574–577
8. Herle PS, Ellis B, Coombs N, Nazar LF (2004) *Nat Mater* 3:147–152
9. Yang L, Jiao L, Miao Y, Yuan H (2010) *J Solid State Electrochem* 14:1001–1005
10. Pan MS, Lin XH, Zhou ZT (2011) *Chem Lett* 40:1087–1088
11. Yang L, Jiao LF, Miao YL, Yuan H (2009) *J Solid State Electrochem* 13(10):1541–1544
12. Liao XZ, He YS, Ma ZF, Zhang XM, Wang L (2007) *J Power Sources* 174:720–725
13. Zhou X, Zhao XB, Yu HM, Hu JZ (2008) *J Inorg Mater* 23(3):587–591
14. Sun CS, Zhang Y, Zhang XJ, Zhou Z (2010) *J Power Sources* 195:3680–3683
15. Lee SB, Cho SH, Aravindan V, Kim HS, Lee YS (2009) *B Kor Chem Soc* 30(10):2223–2226
16. Wang D, Li H, Wang Z, Wu X, Sun Y, Huang X, Chen L (2004) *J Solid State Chem* 177:4582–4587
17. Zhong ME, Zhou ZT (2010) *Mater Chem Phys* 119:428–431
18. Wang L, Liang GC, Ou XQ, Zhi XK, Zhang JP, Cui JY (2009) *J Power Sources* 189:423–428
19. Barker J, Saidi MY, Swoyer JL (2003) *Electrochem Solid-State Lett* 6(3):A53–A55
20. Liu AF, Hu ZH, Wen ZB, Lei L, An J (2010) *Ionics* 16(4):311–316
21. Prosini PP, Lisi M, Zane D, Pasquali M (2002) *Solid State Ionics* 148:45–51